JOURNAL OF CATALYSIS 144, 214–226 (1993)

Alcohol Decomposition by Reverse Spillover

BAOSHU CHEN AND JOHN L. FALCONER

Department of Chemical Engineering, University of Colorado, Boulder, Colorado 80309-0424

Received February 22, 1993; revised June 6, 1993

Temperature-programmed desorption (TPD) was used to study methanol, ethanol, and 1-propanol decomposition on Al_2O_3 and Ni/Al_2O_3 catalysts. These alcohols adsorb on the Al_2O_3 support of Ni/Al_2O_3 and dehydrogenate by reverse spillover to the Ni surface. Thus, the presence of Ni dramatically increases their decomposition rates. Methanol adsorbed on Al_2O_3 alone decomposes to form $(CH_3)_2O$ at lower temperature and CO, H_2, and CO_2 above 600 K. On Ni/Al_2O_3, most CH_3OH dehydrogenates to form CO and H_2. Ethanol adsorbed on Al_2O_3 mostly dehydrates to form C_2H_4 and $(C_2H_5)_2O$, but C_2H_4O and H_2 are also observed. On Ni/Al_2O_3, C_2H_5OH dehydrogenation to CO, H_2, and surface carbon is the main reaction. 1-Propanol decomposes on Al_2O_3 to form C_3H_6, H_2, $(C_3H_7)_2O$, and C_3H_6O. When Ni is present, propanol decomposition to H_2, CO, and surface carbon is the dominant process, but some C_3H_6, C_3H_6O, and CO_2 also form. On Al_2O_3, the alcohols decomposition rates are in the order $1\text{-}C_3H_7OH > C_2H_5OH > CH_3OH$, but on Ni/Al_2O_3 the rates are almost identical. The increase in the decomposition rate of alcohols, when Ni is present, is attributed to alcohol diffusion along the Al_2O_3 surface and decomposition on the Ni surface or at the $Ni\text{–}Al_2O_3$ interface. The diffusivity of CH_3O on the Al_2O_3 surface at 534 K is estimated to be larger than 6.6×10^{-11} cm^2/s.

INTRODUCTION

Alcohols dehydrate on Al_2O_3 surfaces to form ethers and olefins (for higher alcohols) (*1*, *2*), and a recent study by Narayanan *et al.* (*3*) concluded that isopropanol dehydration takes place by surface diffusion to a small concentration of active sites on the Al_2O_3 surface. They varied the active site concentration, and thus the dehydration rate, by using a series of Al_2O_3 catalysts with different concentrations of impurities. In the present study, we show that a similar process occurs for methanol, ethanol, and 1-propanol *dehydrogenation* on Ni/Al_2O_3 catalysts.

Temperature-programmed desorption (TPD) was used to compare dehydrogenation rates on Al_2O_3 and on Ni/Al_2O_3. These experiments show that the presence of Ni dramatically increases the rate of alcohol decomposition. TPD allows for a direct comparison between the two catalysts because the alcohols mostly adsorb on the Al_2O_3 surface for both catalysts. The TPD was carried out to sufficiently high temperature that the dehydrogenation rates were measured for both catalysts.

On Al_2O_3 catalysts, alcohols dehydrate to form ethers, olefins, and aldehydes (for higher alcohols), but dehydrogenation is also observed (*4*). On nickel, alcohols dehydrogenate much more readily, so that both the reaction rate and the reaction products formed during TPD can be used to determine how important surface diffusion is for alcohol decomposition on supported nickel. Nickel surfaces in UHV are so active for alcohol decomposition that methanol decomposes to CO and H_2 at 290 K, and the appearances of CO and H_2 in the gas phase are then limited by their desorption properties (*5*, *6*). Since most of the alcohols adsorbed at 300 K are on the Al_2O_3 support in the current study, the Ni can only be important in the reaction process if the alcohols diffuse to the Ni particles and undergo reverse spillover. To determine the fate of the hydroxyl hydrogen in methanol, TPD of CH_3OD adsorbed on Ni/Al_2O_3 was also carried out.

0021-9517/93 $5.00

EXPERIMENTAL METHODS

Temperature-programmed desorption (TPD) experiments were carried out on a 5.7% Ni/Al_2O_3 catalyst and on Kaiser A-201 Al_2O_3 at ambient pressure in a flow system that has been described previously (*7–9*). A 100-mg catalyst sample (60–80 mesh) was supported on a quartz frit in a 1-cm OD quartz reactor, which was placed in an electric furnace. A 0.5-mm OD, chromel-alumel shielded thermocouple, which was centered in the catalyst bed, was connected to a temperature programmer to control the furnace to provide a constant heating rate of 1 K/s. The carrier gases (He, H_2, and Ar) at atmospheric pressure flowed over the catalyst at a flowrate of 100 cm^2/min (STP). Immediately downstream, the gas was analyzed with a UTI quadrupole mass spectrometer located in a turbopumped ultra-high-vacuum system. A computer allowed detection of multiple mass signals.

The reduced and passivated Ni/Al_2O_3 catalyst was pretreated for 2 h at 773 K in H_2 flow, and then the carrier gas was switched to He before the catalyst was cooled to room temperature. For consistency, the Al_2O_3 catalyst was also pretreated for 2 h at 773 K in H_2 flow and cooled in He flow. Alcohol (2 μl liquid) was injected slowly at 300 K by a liquid syringe into the He carrier gas upstream of the reactor. After the catalyst was held for 30 min at 300 K in He flow for equilibration, TPD was carried out by heating the catalyst in He flow at a rate of 1 K/s. In one series of experiments, CH_3OD (3 μl) was adsorbed at 300 K on Ni/Al_2O_3, and TPD was carried out in Ar flow so that D_2 signals could be detected. The final temperature during TPD was 900 K for Al_2O_3 and 773 K for Ni/Al_2O_3. In one experiment, however, following C_2H_5OH adsorption on Ni/Al_2O_3, the temperature was increased to 950 K, but the catalyst was not used further because of sintering.

During TPD following CH_3OH adsorption, H_2, CH_4(m/z = 15,16), H_2O, CO, CH_2O(29), CH_3OH(31,32), CO_2, and $(CH_3)_2O$(45,46) were detected. The mass 31 signal was first corrected for cracking of $(CH_3)_2O$, and the remaining mass 31 signal was due to CH_3OH. The cracking fractions at mass 28 from CO_2, CH_3OH, and $(CH_3)_2O$ were subtracted from the mass 28 signal to obtain the CO signal. Similarly, the signals at masses 2, 15, and 29 were corrected for cracking of CH_3OH and $(CH_3)_2O$ to obtain H_2, CH_4, and CH_2O signals, respectively. Masses 16 and 32 were also monitored to identify the formation of CH_4 and CH_3OH, respectively. During TPD of CH_3OD, H_2, HD(3), D_2(4), CH_4, CH_3D(17), H_2O, HDO(19), CO, CH_3OH, CH_3OD(33), CO_2, and $(CH_3)_2O$ were monitored. The mass 17 signal was corrected for cracking of H_2O to obtain the CH_3D signal. The corrections for masses 15, 28, and 31 are similar to those during TPD of CH_3OH.

For TPD of C_2H_5OH, in addition to signals for H_2, CH_4, H_2O, CO and CO_2, signals for C_2H_4(26), C_2H_6(30), C_2H_4O(29,43), C_2H_5OH(31,46), and $(C_2H_5)_2O$(59,74) were also detected. Mass 28 signals were corrected for cracking of CO_2, C_2H_4, C_2H_6, and C_2H_5OH to obtain CO signals. Mass 32 was also monitored to determine if CH_3OH forms and contributes to the mass 31 signal. For TPD of 1-C_3H_7OH, H_2, CO, CH_4, CO_2, H_2O, C_3H_6(41), C_3H_6O(29), and $(C_3H_7)_2O$(43,73) were detected. To calibrate the mass spectrometer, known volumes of pure gases or liquids were injected into the He or Ar carrier gas, downstream of the reactor. The calibration factor for CO was used to estimate the C_2H_4O and C_3H_4O desorption rates, and the calibration factor for $(CH_3)_2O$ was used to estimate $(C_2H_5)_2O$ and $(C_3H_7)_2O$ formation rates.

The Al_2O_3, Kaiser A-201, was heated at 773 K in air for 10 h prior to loading in the TPD reactor. The 5.7% Ni/Al_2O_3 catalyst was prepared by impregnating Kaiser Al_2O_3 (A-201) to incipient wetness with an aqueous solution of nickel nitrate. After being dried in a vacuum oven for 24 h at 373–383 K, the catalyst was directly reduced in H_2 for 10 h at 773 K and passivated with 2% O_2 in N_2 at room temperature. The weight

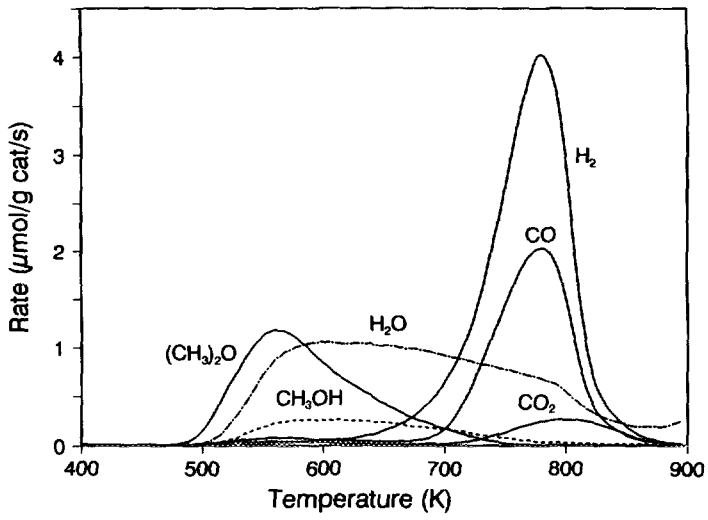

FIG. 1. TPD spectra of CH_3OH (2 μl) adsorbed at 300 K on Al_2O_3.

loading was measured by inductively coupled plasma mass spectrometry. The dispersion and the surface area of Ni are 1.7% and 0.6 m^2/g catalyst, respectively, and they were estimated by temperature-programmed reaction in H_2 flow of adsorbed CO (*10*).

RESULTS

Methanol Decomposition

Figure 1 shows the products that formed when CH_3OH, adsorbed at 300 K in He flow on Al_2O_3, decomposed during TPD. Methanol desorbed in a broad peak from 500 to 800 K. Methanol dehydration formed $(CH_3)_2O$, which has a maximum rate of formation at 563 K and a high temperature tail. Water started forming near 500 K and was detected up to 900 K. Above 650 K, most of the adsorbed CH_3OH decomposed to form CO and H_2 simultaneously (peak temperature of 780 K). A small amount of CO_2 also formed above 700 K. No significant amounts of CH_4 and CH_2O were detected. The ratio of $H/(CO + CO_2)$ from the high temperature CO, H_2, and CO_2 peaks is 3.4, and the ratio of total H to total C is 4.3. Some of the OH groups on Al_2O_3 reacted to form H_2O above the pretreatment temperature of 773 K. When Al_2O_3 was exposed to CH_3OD in Ar at 300 K, a similar decomposition process was observed during TPD in Ar flow. The CO, H_2, HD, and D_2 all formed simultaneously in single peaks with maxima at 780 K. Also, CH_3OH, CH_3OD, H_2O, and HDO were detected.

When Ni/Al_2O_3 was exposed to CH_3OH at 300 K, almost all the CH_3OH adsorbed on the Al_2O_3 surface, but the reaction rate and the product distribution were quite different, as shown in Fig. 2. The main desorbing species were CO and H_2 and they formed simultaneously with a $H/(CO + CO_2)$ ratio of 3.7. Only small amounts of CH_4, H_2O, $(CH_3)_2O$, and CO_2 were detected. That is, dehydrogenation of CH_3OH to CO and H_2 was the dominant decomposition process on Ni/Al_2O_3. The important point to note is that the peak temperature for CO and H_2 formation on Ni/Al_2O_3 is approximately 530 K. In contrast, the peak temperature for $(CH_3)_2O$ formation on Al_2O_3 (Fig. 1) was 563 K, and CO and H_2 only started forming above 600 K on Al_2O_3. The CO and H_2 peaks at 780 K in Fig. 1 are absent in Fig. 2 because CH_3OH decomposed much faster when Ni was present. The amounts and peak temperatures of products are in Table 1.

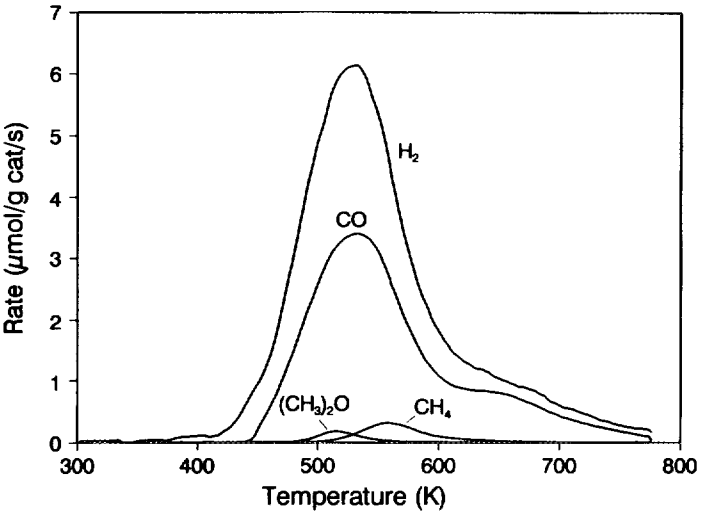

FIG. 2. TPD spectra of CH_3OH (2 μl) adsorbed at 300 K on 5.7% Ni/Al_2O_3.

Following exposure of Ni/Al_2O_3 at 300 K to CH_3OD, TPD in Ar flow showed that HD and D_2 desorbed at almost the same temperature as H_2 and CO (Fig. 3). Some HDO desorbed from 400 to 800 K with the same peak shape as H_2O. These are not shown in Fig. 3 for clarity. The H/D and (H + D)/CO ratios are 5 and 3.5, respectively. Both CH_3OH and CH_3OD desorbed with peak temperatures of 460 K. The amount and peak shape of CH_3OD are similar to those of CH_3OH, but the CH_3OD peak is not shown in Fig. 3 for clarity. Dimethyl ether were detected with peak temperature of 520 K. A small amount of CO_2 also desorbed above 600 K.

TABLE 1

TPD of CH_3OH on Al_2O_3 and Ni/Al_2O_3

Products	Peak temperatures (K)		Amounts desorbed (μmol/g catalyst)	
	Al_2O_3	Ni/Al_2O_3	Al_2O_3	Ni/Al_2O_3
CO	777	534	172	410
H_2	779	528	334	777
$(CH_3)_2O$	563	514	133	10
CH_4	—	554	—	23
CO_2	809	718	26	12
H_2O	—	—	271	9.5
Total carbon			464	465
(Total H)/4			502	431

Ethanol Decomposition

In contrast to CH_3OH, C_2H_5OH decomposed on Al_2O_3 almost completely by 700 K, and as shown in Fig. 4 the dominant process was dehydration to C_2H_4. A large amount of H_2O was also observed (Table 2). Smaller amounts of H_2, $(C_2H_5)_2O$, and C_2H_4O were detected. The amounts of CO, C_2H_6, and CH_4 were insignificant, and no unreacted C_2H_5OH desorbed.

Ethanol decomposition on Ni/Al_2O_3 was quite different. On Al_2O_3, all the products were observed between 525 and 700 K, but as shown in Fig. 5 for Ni/Al_2O_3, products desorbed from 400 to 925 K. Moreover, C_2H_5OH dehydrogenation to H_2 and CO was the dominant process and this occurred over the entire temperature range. Smaller amounts of C_2H_4, C_2H_4O, CH_4, CO_2, and H_2O were also observed. The product amounts and peak temperatures are compared for the two catalysts in Table 2.

1-Propanol Decomposition

1-Propanol decomposition on Al_2O_3 was similar to C_2H_5OH decomposition. The

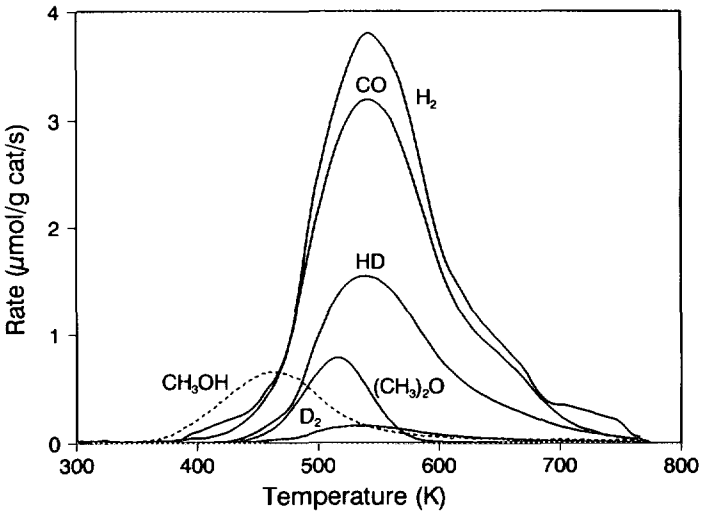

FIG. 3. TPD spectra of CH_3OD (3 μl) adsorbed at 300 K on 5.7% Ni/Al_2O_3.

main reaction was dehydration to form C_3H_6 and H_2O (Fig. 6). Propylene formed in a single peak with a maximum at 625 K, and H_2O started forming at 550 K and was detected up to 900 K. Smaller amounts of H_2, $(C_3H_7)_2O$, and C_3H_6O desorbed in single peaks from 500 to 800 K (Table 3). Significant amounts of CO, CO_2, C_3H_8, and C_3H_7OH were not detected.

On Ni/Al_2O_3, decomposition of 1-C_3H_7OH was faster, and much more dehydrogenation took place (Fig. 7). Propylene also formed in a peak at 562 K, which is 63 K lower than on Al_2O_3. Starting near 400 K, dehydrogenation to CO and H_2 was the dominant reaction on Ni/Al_2O_3. Starting near 400 K, dehydrogenation to CO and H_2 was the dominant reaction on Ni/Al_2O_3, and

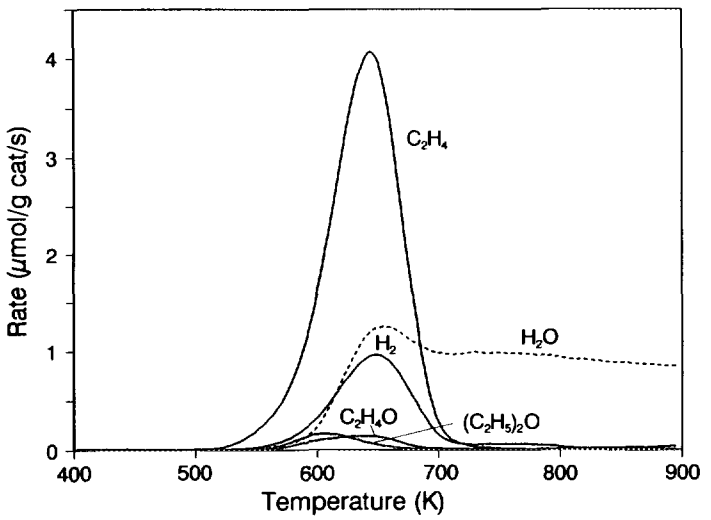

FIG. 4. TPD spectra of C_2H_5OH (2 μl) adsorbed at 300 K on Al_2O_3.

TABLE 2

TPD of C_2H_5OH on Al_2O_3 and Ni/Al_2O_3

Products	Peak temperatures (K)		Amounts desorbed (μmol/g catalyst)	
	Al_2O_3	Ni/Al_2O_3	Al_2O_3	Ni/Al_2O_3
CO	—	500	—	380
CH_4	—	500	87	49
H_2	648	523	87	683
$(C_2H_5)_2O$	600	—	14	—
C_2H_4	646	579	301	64
C_2H_4O	650	574	15	17
CO_2	—	750	—	24
H_2O	—	—	293	47
Total carbon			775	615
(Total H)/3			837	660

CO and H_2 continued to form to 773 K, the highest temperature reached. Small amounts of C_3H_6O and CO_2 were also observed. The peak temperatures and the amounts of each product are given in Table 3.

DISCUSSION

Reverse Spillover

A comparison of the TPD results for Ni/Al_2O_3 and Al_2O_3 shows that a small concentration of Ni dramatically changes the decomposition properties of methanol, ethanol, and 1-propanol on Al_2O_3. As shown in Tables 1–3, the amounts of each alcohol adsorbed are similar for both catalysts because almost all the alcohol adsorbs on the Al_2O_3 surface. Thus, in order for the decomposition of the alcohol adsorbed on the Al_2O_3 to be affected by the Ni, the alcohol or the species that form upon adsorption must diffuse to the Ni crystallites. Decomposition on Ni/Al_2O_3 thus takes place by reverse spillover to the $Ni–Al_2O_3$ interface or the Ni surface, which is a more active dehydrogenation catalyst than the Al_2O_3 surface. Several aspects of the TPD data indicate that surface diffusion is responsible for the decomposition.

- The rate of decomposition increases dramatically when Ni is present.
- Dehydrogenation to CO and H_2 increases when Ni is present because Ni is a good dehydrogenation catalyst but Al_2O_3 is not.
- The rate of alcohol decomposition on Al_2O_3 is in the order $1\text{-}C_3H_7OH > C_2H_5OH > CH_3OH$, but on Ni/Al_2O_3 the alcohols decompose at essentially the same rate.

TPD is effective for studying this reverse spillover because it essentially measures the

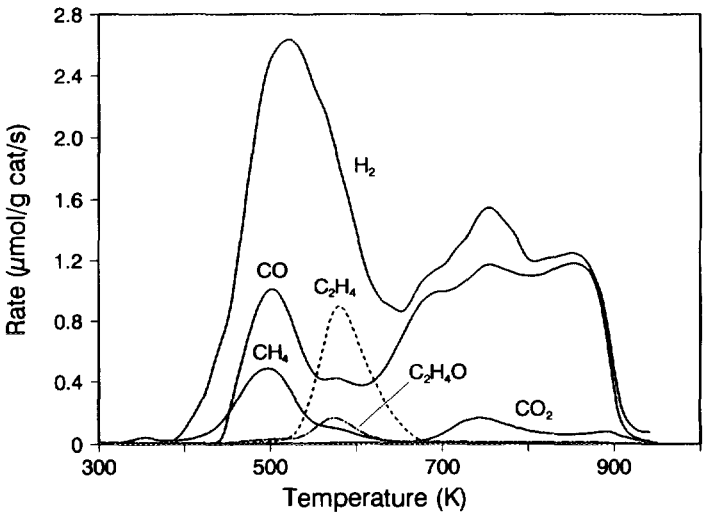

FIG. 5. TPD spectra of C_2H_5OH (2 μl) adsorbed at 300 K on 5.7% Ni/Al_2O_3.

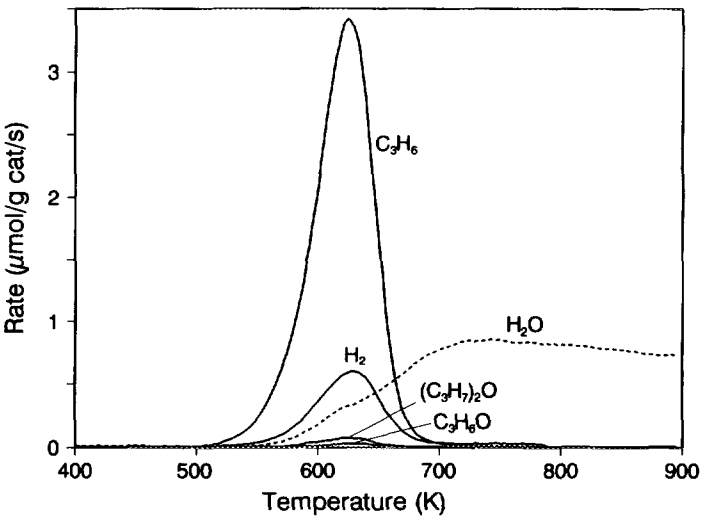

FIG. 6. TPD spectra of 1-C_3H_7OH (2 μl) adsorbed at 300 K on Al_2O_3.

specific rate of reaction. Because the alcohol does not decompose or desorb until higher temperatures in the absence of Ni, the enhanced decomposition rate is not due to desorption from Al_2O_3 and readsorption on Ni. Instead, the fact that CO and H_2 desorbed simultaneously from Ni/Al_2O_3 shows that their formation was limited either by the rate of reverse spillover or the rate of decomposition of an adsorbed species on Ni or at the $Ni\text{-}Al_2O_3$ interface.

The Ni surface area (0.6 m^2/g catalyst) was estimated by hydrogenating CO (adsorbed at 300 K) to form CH_4 during temperature-programmed reaction (*10*). Since the BET surface area of Kaiser A-201 Al_2O_3 is 220 m^2/g Al_2O_3 (*1*), almost no alcohol is adsorbed on Ni, but most of the alcohol decomposes on the Ni surface or at the $Ni\text{-}Al_2O_3$ interface. Because the Ni surface is so active for alcohol decomposition, relative to Al_2O_3, most of the alcohol probably decomposes as soon as it spills over to Ni from Al_2O_3.

Narayanan *et al.* (*3*) concluded that surface diffusion was necessary for isopropanol decomposition on Al_2O_3 because only a small fraction of the surface sites was active for decomposition. Our results for Ni/Al_2O_3 show that when a small number of active Ni sites are placed on the Al_2O_3 surface, alcohols diffuse to the Ni surfaces and react. The formation of HD and D_2 during TPD of CH_3OD on Ni/Al_2O_3 (Fig. 3) suggests that CH_3O species diffuse along the Al_2O_3 surface together with D or H of the adjacent OD or OH groups. The CH_3OD adsorbed on Al_2O_3 to form CH_3O and OD. On the Ni surface or at the $Ni\text{-}Al_2O_3$ interface, CH_3O and OD or OH decomposed to form CO, H_2, HD, and D_2. Theoretical analysis by Anderson and Jen (*11*) suggested that CH_3O moved as an anion from one Al^{3+} site to another, paired with a proton, which moved from one O^{2-} site to another. The results for CH_3OD decomposition are consistent with this model. For clarity, CH_3O is used to represent the diffusing species during CH_3OH decomposition in the following discussion.

Previous TPD studies for CH_3OH adsorption on Pt/Al_2O_3 (*12*) showed similar results to our TPD of CH_3OH on Ni/Al_2O_3 (Fig. 2). Methanol, which adsorbed on the Al_2O_3 surface of Pt/Al_2O_3, decomposed to form CO and H_2 simultaneously with a peak temperature near 500 K (*12*). During TPD after CO and H_2 were coadsorbed at 385 K on Pt/Al_2O_3 (*12*) and Pd/Al_2O_3 (*13*), CO and H_2 also desorbed simultaneously in single

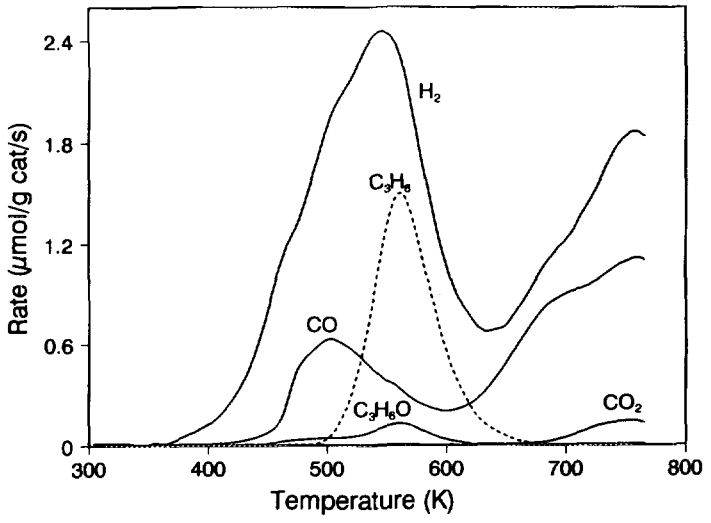

FIG. 7. TPD spectra of 1-C_3H_7OH (2 μl) adsorbed at 300 K on 5.7% Ni/Al_2O_3.

peaks at 500 K. In those experiments, CH_3O formed on Al_2O_3 during CO and H_2 coadsorption at 385 K. The similarity of TPD for CH_3OH on Ni/Al_2O_3, CH_3OH on Pt/Al_2O_3, and CH_3O on Pt/Al_2O_3 and Pd/Al_2O_3 indicates that the increased decomposition rate of CH_3OH on Ni/Al_2O_3, relative to that on Al_2O_3 alone, is due to reverse spillover of CH_3OH, and is not due to additional reaction sites created by the formation of Ni aluminate on the support.

TABLE 3

TPD of 1-C_3H_7OH on Al_2O_3 and Ni/Al_2O_3

Products	Peak temperatures (K)		Amounts desorbed (μmol/g catalyst)	
	Al_2O_3	Ni/Al_2O_3	Al_2O_3	Ni/Al_2O_3
CO	—	504	—	>186
H_2	631	546	44	>477
$(C_3H_7)_2O$	625	—	8	—
C_3H_6	625	562	215	93
C_3H_6O	623	562	6	13
CO_2	—	504	—	>13
H_2O	—	—	220	>41
Total carbon			711	>517
(Total H) × 3/8			737	>627

Another possible explanation for the increased rate of alcohol decomposition is that H_2 spillover, during treatment in H_2 at 773 K, created new types of active sites on the Al_2O_3 surface. Teichner (*14*) observed that active sites were created on the Al_2O_3 phase of a Pt/Al_2O_3 + Al_2O_3 mixture by H_2 gas exposure at 673 K. These sites on Al_2O_3 were active for ethylene hydrogenation, even when the Pt/Al_2O_3 was subsequently separated from the Al_2O_3. To determine whether this type activation was responsible for the increased rate of alcohol decomposition that we observed, a reactor was used in which 50 mg of Ni/Al_2O_3 was placed on top of 50 mg of Al_2O_3. The mixture was pretreated for 30 min in H_2 at 773 K, and then TPD of CH_3OH (500 μmol/g mixture) was carried out. Hydrogen and CO products formed in two distinct processes, with peak maxima at 525 and 780 K, and some $(CH_3)_2O$, CO_2, and CH_4 formed. The low temperature peaks were similar to the corresponding peaks in Fig. 2 for TPD of CH_3OH on Ni/Al_2O_3, and the high temperature peaks were similar to those in Fig. 1 for TPD of CH_3OH on Al_2O_3. The same results were obtained if the mixture was pretreated for 4 h in H_2 at 773 K. Thus, treatment in H_2 did not appear to activate the Al_2O_3 support

for alcohol decomposition, and instead reverse spillover of alcohol from Al_2O_3 to Ni is responsible for alcohol decomposition. Our previous studies (*15*) also showed that following CH_3OH adsorption on Ni/Al_2O_3, isothermal treatment at 425 K in He caused reverse spillover and CO was formed on the Ni. This further supports our explanation as to why Ni increases the rate of alcohol decomposition.

Comparison of Rates

Both peak width analysis (*16, 17*) and Redhead's analysis (*18, 19*) were used to estimate activation energies for CO and H_2 formation on the catalysts. Though these methods are subject to significant errors, particularly if surface diffusion is the limiting step, they are useful for comparing relative rate constants, which were calculated from the activation energies and preexponential factors. Estimates based on the H_2 peak temperatures show that at 600 K, Ni increased the rate of methanol decomposition between a factor of 10^5 (Redhead's analysis) and 10^7 (peak width analysis), the rate of ethanol decomposition between a factor of 10^3 (Redhead's analysis) and 10^5 (peak width analysis), and the rate of 1-propanol decomposition a factor of 10^2 (Redhead's analysis). The broad H_2 peak in Fig. 7 could not be analyzed by peak width analysis. These rate increases for dehydrogenation correspond to decreases in peak temperature of 250 K for methanol, 125 K for ethanol, and 85 K for 1-propanol. The presence of Ni also increased the rate of C_2H_5OH dehydration approximately a factor of 50 and the rate of 1-C_3H_7OH dehydrogenation a factor of 40 at 600 K.

The initial rates of H_2 and CO formation on Ni/Al_2O_3 from C_2H_5OH and 1-C_3H_7OH were similar to those from CH_3OH, but CO and H_2 from C_2H_5OH decomposition continued to form up to 900 K, and CO and H_2 from 1-C_3H_7OH decomposition still formed above 775 K. On Al_2O_3 alone, C_2H_5OH and 1-C_3H_7OH decompositions (Figs. 4 and 6) instead were complete by 700 K. The high temperature CO from C_2H_5OH and 1-C_3H_7OH decomposition on Ni/Al_2O_3 probably resulted from an intermediate adsorbed species that formed on the Ni surface, possibly a CH_x species. This CH_x species then reacted with surface oxygen at high temperature to form CO and H_2 on Ni/Al_2O_3. Gates *et al.* (*20*) detected surface carbon in addition to CH_4, CO, H_2, and C_2H_4O when C_2H_5OH decomposed on Ni(111). The C–C bond is easier to break than the C–H in the CH_3 group (*20*). The similarity of CH_3OH, C_2H_5OH, and 1-C_3H_7OH initial decomposition rates indicates that their rates are probably limited by the same step such as spillover from Al_2O_3 to Ni. The rate of spillover might not be expected to be different for similar molecules. Decomposition to CO and H_2, which occurs after spillover, is expected to be fast because CH_3OH has been reported to decompose on Ni at 290 K to form CO and H_2 (*6, 21*). Since CO and H_2 do not form until much higher temperature in Fig. 2, CH_3OH decomposition on Ni does not limit CO and H_2 formation.

For uniformed-size, spherical Ni particles and complete Ni reduction, the Ni particles are calculated to be 60 nm in diameter and the average distance between two adjacent particles is then approximately 1400 nm. This means the maximum distance that a molecule would have to diffuse to decompose is 700 nm. These estimates are based on Ni and Al_2O_3 surface areas, and are approximate since the Ni is not completely reduced. The diffusion distance of CH_3O adsorbed on Al_2O_3 also can be estimated using the model of Boudart and co-workers (*22, 23*),

$$X_D = (a/2)\exp[(E_d - E_D)/(2RT)],$$

where X_D is the distance CH_3O diffuses before it desorbs, a is the hop distance for surface diffusion, R is the gas constant, E_D and E_d are the activation energies for CH_3O diffusion on and desorption from Al_2O_3, respectively, and T is temperature. At 534 K, which is the CO peak temperature for CH_3OH decomposition on Ni/Al_2O_3, sur-

face diffusion of CH_3O on the Al_2O_3 surface of Ni/Al_2O_3 was assumed to be the rate-determining step in order to estimate the distance. This estimate will then give a lower estimate of diffusivity if spillover is limiting. The activation energy for CO formation from CH_3OH on Ni/Al_2O_3 is E_D, and E_d is the activation energy of CO formation from CH_3OH decomposition on Al_2O_3 alone. If $a = 0.4$ nm is used (*22*), then X_D is estimated to be 470 nm. This value is close to the value of 700 nm obtained by using Ni surface area. Since CH_3O reverse spillover from Al_2O_3 to Ni limits CH_3OH decomposition, the rate of CH_3O diffusion is faster than the apparent rate of CO formation.

For CH_3OH decomposition on Ni/Al_2O_3, if diffusion of CH_3OH on Al_2O_3 is the rate-determining step, the concentration of CH_3OH on the Ni surface or at the $Ni–Al_2O_3$ interface will be much lower than that on the Al_2O_3 surface, and the rate of surface diffusion will be the same as the CO formation rate. From TPD of CH_3OH (Fig. 2), the CO formation rate at 534 K is 3.4 μmol/g catalyst/s. Thus, the diffusivity of CH_3O on the Al_2O_3 surface is estimated to be 6.6×10^{-11} cm^2/s according to Fick's law (*24*). This will be a lower estimate, however, if surface diffusion of CH_3O is not the rate-determining step during CH_3OH dehydrogenation.

Methanol Decomposition on Al_2O_3

Previous studies (*25–28*) with IR and microcalorimetry on pure Al_2O_3 following CH_3OH adsorption showed two types of adsorbed species: strongly adsorbed CH_3OH on basic sites and surface CH_3O species on Lewis acid sites. The CH_3O groups were the only irreversibly adsorbed species above 443 K (*26, 27*). In the present TPD experiment, since CH_3OH desorbs from 500 to 800 K (Fig. 1), its formation is probably due to the recombination of adsorbed CH_3O species with a proton from a hydroxyl group on Al_2O_3.

Two mechanisms have been proposed in previous studies to explain $(CH_3)_2O$ formation from CH_3OH (*2, 4, 29*). Jain and Pillai (*29*) suggested that $(CH_3)_2O$ formed by a bimolecular reaction between a CH_3O species and a strongly adsorbed CH_3OH. Similar models were developed by Padmanabhan and Eastburn (*30*) and Knözinger *et al.* (*31*). Matsushima and White (*4*) proposed, however, that dimethyl ether formed through the interaction of two adsorbed CH_3O species. They observed that in the presence of gas-phase CD_3OD the ether produced by thermal desorption from an Al_2O_3 surface on which CH_3OH had been preadsorbed was primarily $(CH_3)_2O$. More recently, DeCanio *et al.* (*2*) detected $(CH_3)_2O$ with a peak maximum at 467 K for CH_3OH dehydration on Al_2O_3, but no physisorbed CH_3OH was detected. They concluded that $(CH_3)_2O$ formed by the reaction between two CH_3O species and not between a CH_3O and a molecularly adsorbed CH_3OH. They did not mention the possibility of CH_3OH formation by the reaction between adsorbed CH_3O and H at elevated temperature. Our $(CH_3)_2O$ peak in Fig. 1 is broader (from 450 to 800 K) and is about 95 K higher than that observed by DeCanio *et al.* (*2*). Part of this difference results because DeCanio *et al.* used a lower heating rate (0.4 K/s), but $(CH_3)_2O$ is also more likely to readsorb in our study and they used a different alumina. Since CH_3OH desorbed over the same temperature range as $(CH_3)_2O$ in the present study, formation of $(CH_3)_2O$ could be due to reaction between adsorbed CH_3O and CH_3OH. The reaction of two CH_3O to form $(CH_3)_2O$ is also possible, since $(CH_3)_2O$ formed during TPD of CH_3OH on Ni/Al_2O_3 although CH_3OH was not observed (Fig. 2).

The formation of CO and H_2 at higher temperature is attributed to the decomposition of CH_3O and OH groups, since H_2 and CO desorb simultaneously and the $H/(CO + CO_2)$ ratio is larger than 3. During TPD of CH_3OD adsorbed on Al_2O_3, HD, D_2, H_2, and CO desorbed simultaneously. Since CH_3OD forms adsorbed CH_3O and OD on Al_2O_3 at 300 K, the formation of HD and D_2 is due to the decomposition of CH_3O and OD

or OH. Carbon dioxide may be produced by CO disproportionation or by the recombination of CO and surface oxygen. Matsushima and White (*4*) also detected CO, H_2, and CO_2 during CH_3OH decomposition on Al_2O_3 at high temperature, but DeCanio et al. (*2*) did not observe the formation of CO, H_2, and CO_2 since they only ran TPD to 650 K.

Because Greenler (*25*) and Kagel (*28*) reported that formate species (HCOO) formed above 450 K from CH_3OH adsorbed on Al_2O_3, TPD following HCOOH adsorption on Al_2O_3 was carried out (*10*). Formic acid decomposed mostly into CO (peak temperature of 525 K) and H_2O, which desorbed at wider temperature range (from 500 K to 775 K). Infrared studies (*32–34*) have identified formation of HCOO species following HCOOH adsorption on Al_2O_3. Since CO and H_2 desorb above 600 K for CH_3OH adsorption (Fig. 1), the formation of formate from CH_3OH seems unlikely under our conditions.

Ethanol Decomposition on Al_2O_3

Previous IR studies (*25, 28, 35*) have shown that C_2H_5OH adsorbs on Al_2O_3 to form C_2H_5O and OH species, and physically adsorbed C_2H_5OH can be removed by evacuation at 343 K (*35*). Formation of $(C_2H_5)_2O$, which desorbed from Al_2O_3 at a similar rate as $(CH_3)_2O$ from CH_3OH decomposition, may be due to the reactions between adsorbed C_2H_5O and C_2H_5OH or between two C_2H_5O species. Ethanol may form by the recombination of C_2H_5O and H and then react with another C_2H_5O to form $(C_2H_5)_2O$. At higher temperature, C_2H_5OH decomposition on Al_2O_3 is different from CH_3OH decomposition. Ethanol decomposes to form C_2H_4, C_2H_4O, and H_2, but CH_3OH decomposes to form CO, H_2, and CO_2. Ethanol also decomposes faster than CH_3OH. Arai *et al.* (*36*) concluded that C_2H_4 formed by the abstraction of a methyl hydrogen by an adjacent exposed oxide ion and the simultaneous rupture of the C–O bond. For C_2H_5OH decomposition on Al_2O_3, $(C_2H_5)_2O$ and C_2H_4 has been detected in several studies (*1, 2, 28, 36*), but the formation of C_2H_4O and H_2, which were observed in the present study, was not reported in those studies. Kim and Barteau (*37*), however, detected C_2H_4O and H_2 during TPD of C_2H_5OH on TiO_2. They attributed C_2H_4O formation to α-H elimination of a C_2H_5O species. Note that H_2 desorbed at the same temperature as C_2H_4 and C_2H_4O during TPD of C_2H_5OH on Al_2O_3 (Fig. 4). Hydrogen may form by the reaction between the hydrogen in the methyl or methylene group of C_2H_5O and surface hydrogen, which may adsorb on weak basic sites adjacent to the C_2H_5O adsorption site.

Note that the C_2H_4 and C_2H_4O peaks from Ni/Al_2O_3 (Fig. 5) are similar to those formed in TPD of C_2H_5OH on Al_2O_3 alone (Fig. 4), and their formation may follow the same mechanism as on Al_2O_3. That is, C_2H_5O decomposes to C_2H_4 and C_2H_4O on Al_2O_3 in parallel with the reverse spillover of C_2H_5O from Al_2O_3 to Ni.

1-Propanol Decomposition on Al_2O_3

Previous IR studies showed that two species formed on the Al_2O_3 surface following 1-C_3H_7OH adsorption on Al_2O_3 up to 450 K (*28, 38*). One was physically adsorbed 1-C_3H_7OH, and another was 1-C_3H_7O. The gaseous product, which formed at 673 K and was detected by mass spectrometry, consisted mainly of C_3H_6 and H_2O (*38*). Thus, C_3H_6 formation was attributed to dehydration of physically adsorbed C_3H_7OH (*38*). DeCanio *et al.* (*2*) detected C_3H_6, H_2O, and $(C_3H_7)_2O$ during TPD of 1-C_3H_7OH adsorbed on Al_2O_3, but they did not observe a significant H_2 signal below 573 K. In the present study, in addition to C_3H_6, H_2O, $(C_3H_7)_2O$, and C_3H_6O, a significant amount of H_2 was detected (Fig. 6). This result is similar to that during TPD of C_2H_5OH decomposition on Al_2O_3 (Fig. 4). Thus, adsorbed C_3H_7O species on Al_2O_3 may decompose to form C_3H_6, C_3H_6O, and H_2 in a mechanism similar to that for C_2H_5O species. Kim and Barteau (*37*) detected similar products (C_3H_6, H_2O, H_2, $(C_3H_7)_2O$, C_3H_6O,

and CO_2) during TPD of 1-C_3H_7OH adsorbed on TiO_2. Because of the similarity between TPD of C_2H_5OH and 1-C_3H_7OH, formation of $(C_3H_7)_2O$ may be due to the reaction between adsorbed 1-C_3H_7OH and 1-C_3H_7O or the reaction between two 1-C_3H_7O species. The decomposition rate of 1-C_3H_7OH on Al_2O_3 is higher than that of C_2H_5OH, and C_2H_5OH decomposes faster than CH_3OH. On TiO_2, Kim and Barteau (*37*) also observed that the rate of alkoxide decomposition was in the order 2-C_3H_7O > 1-C_3H_7O > C_2H_5O > CH_3O. We have also studied TPD of 2-C_3H_7OH on Al_2O_3 and observed that 2-C_3H_7OH decomposes faster than 1-C_3H_7OH. Thus, for the four alcohols studied, we see the same order of reactivity on Al_2O_3 that Kim and Barteau observed on TiO_2 in UHV.

CONCLUSIONS

Methanol adsorbed on Al_2O_3 decomposes to form $(CH_3)_2O$ at low temperature, and to form CO, H_2, and CO_2 above 600 K. The presence of Ni on Al_2O_3 increases the rate of CH_3OH decomposition between a factor of 10^5 and 10^7, and dehydrogenation of CH_3OH to CO and H_2 becomes the dominant process. Ethanol adsorbed on Al_2O_3 mostly dehydrates to form C_2H_4, but smaller amounts of $(C_2H_5)_2O$, C_2H_4O, and H_2 also form. On Ni/Al_2O_3, C_2H_5OH decomposition is 10^3 to 10^5 times faster and the main reaction is dehydrogenation to CO, H_2, and CH_x. 1-Propanol decomposes on Al_2O_3 mostly to form C_3H_6 and H_2O, but some H_2, $(C_3H_7)_2O$, and C_3H_6O were also detected. The presence of Ni on Al_2O_3 increases the rate of 1-C_3H_7OH decomposition a factor of 10^2, and 1-C_3H_7OH decomposition to H_2, CO, and CH_x is the main reaction. All alcohols studied initially decompose to CO and H_2 on Ni/Al_2O_3 at a similar rate though their rates of decomposition are different on Al_2O_3. The increase in the decomposition rate of alcohols, when Ni is present, is attributed to alcohol diffusion along the Al_2O_3 surface, reverse spillover to the Ni–Al_2O_3 interface, and decomposition on the Ni surface or at the interface. The diffusivity of CH_3O on the Al_2O_3 surface at 534 K is estimated to be larger than 6.6×10^{-11} cm^2/s.

ACKNOWLEDGMENTS

We gratefully acknowledge support by the National Science Foundation, Grant CTS-9021194. We also thank Eric M. Cordi for his suggestions concerning the surface diffusion calculations.

REFERENCES

1. Swecker, J. L., and Datye, A. K., *J. Catal.* **121,** 196 (1990).
2. DeCanio, E. C., Nero, V. P., and Bruno, J. W., *J. Catal.* **135,** 444 (1992).
3. Narayanan, C. R., Srinivasan, S., Datye, A. K., Gorte, R., and Biaglow, A., *J. Catal.* **138,** 659 (1992).
4. Matsushima, T., and White, J. M., *J. Catal.* **44,** 183 (1976).
5. Gates, S. M., Russell, J. N., Jr., and Yates, J. T., Jr., *Surf. Sci.* **146,** 199 (1984).
6. Gates, S. M., Russell, J. N., Jr., and Yates, J. T., Jr., *Surf. Sci.* **159,** 233 (1985).
7. Kester, K. B., and Falconer, J. L., *J. Catal.* **89,** 380 (1984).
8. Glugla, P. G., Bailey, K. M., and Falconer, J. L., *J. Phys. Chem.* **92,** 4474 (1988).
9. Schwarz, J. A., and Falconer, J. L., *Catal. Today* **7,** 1 (1990).
10. Chen, B., and Falconer, J. L., submitted to *J. Catal.*
11. Anderson, A. B., and Jen, S., *J. Phys. Chem.* **95,** 7792 (1991).
12. Flesner, R. L., and Falconer, J. L., *J. Catal.* **139,** 421 (1993).
13. Hsiao, E. C., and Falconer, J. L., *J. Catal.* **132,** 145 (1991).
14. Teichner, S. J., *Appl. Catal.* **62,** 1 (1990).
15. Chen, B., Falconer, J. L., and Chang, L., *J. Catal.* **127,** 732 (1991).
16. Chan, C. M., Aris, R., and Weinberg, W. H., *Appl. Surf. Sci.* **4,** 234 (1980).
17. Chan, C. M., and Weinberg, W. H., *Appl. Surf. Sci.* **1,** 377 (1978).
18. Redhead, P. A., *Vacuum* **12,** 203 (1962).
19. Falconer, J. L., and Madix, R. J., *Surf. Sci.* **48,** 393 (1975).
20. Gates, S. M., Russell, J. N., Jr., and Hates, J. T., Jr., *Surg. Sci.* **171,** 111 (1986).
21. Richter, L. J., Gurney, B. A., Villarrubia, J. S., and Ho, W., *Chem. Phys. Lett.* **111,** 185 (1984).
22. Rumpf, F., Poppa, H., and Boudart, M., *Langmuir* **4,** 722 (1988).
23. Kieken, L., and Boudart, M., *in* "Proceedings of

the 10th International Congress on Catalysis, Budapart, Hungary, 1992," to appear.
24. Kapoor, A., Yang, R. T., and Wong, C., *Catal. Rev.-Sci. Eng.* **31,** 129 (1989).
25. Greenler, R. G., *J. Chem. Phys.* **37,** 2094 (1962).
26. Busca, G., Rossi, P. F., and Lorenzelli, V., *J. Phys. Chem.* **89,** 5433 (1985).
27. Rossi, P. F., Busca, G., and Lorenzelli, V., *Z. Phys. Chem.* **149,** 99 (1986).
28. Kagel, R. O., *J. Phys. Chem.* **71,** 844 (1967).
29. Jain, J. R., and Pillai, C. N., *J. Catal.* **9,** 322 (1967).
30. Padmanabhan, V. R., and Eastburn, F. J., *J. Catal.* **24,** 88 (1972).
31. Knözinger, H., Kochloefl, K., and Meye, W., *J. Catal.* **28,** 69 (1973).
32. Koga, O., Onishi, T., and Tamaru, K., *J. Chem. Soc. Chem. Commun.*, 464 (1974).
33. Amenomiya, Y., *Appl. Spectrosc.* **32,** 484 (1978).
34. Amenomiya, Y., *J. Catal.* **57,** 64 (1979).
35. Arai, H., Saito, Y., and Yoneda, Y., *Bull. Chem. Soc. Jpn.* **40,** 731 (1967).
36. Arai, H., Take, J., Saito, Y., and Yoneda, Y., *J. Catal.* **9,** 146 (1967).
37. Kim, K. S., and Barteau, M. A., *Langmuir* **4,** 533 (1988).
38. Deo, A. V., and Dalla Lana, I. G., *J. Phys. Chem.* **73,** 716 (1969).